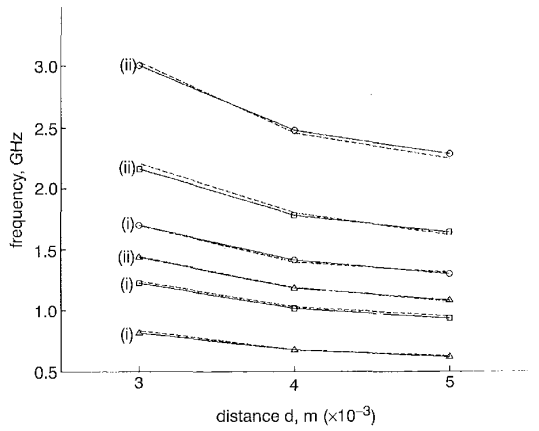

Fig. 3 *Variation of TM_{11} and TM_{21} mode frequencies with distance between centres of arcs for different ε_r and h ($r_1 = 0.04$ m, $r_2 = 0.06$ m)*

---- experimental
—— theoretical
○ $\varepsilon_r = 2.2$, $h = 0.0008$ m
△ $\varepsilon_r = 10.2$, $h = 0.00066$ m
□ $\varepsilon_r = 4.28$, $h = 0.0016$ m
(i) f_{11}
(ii) f_{21}

Conclusion: Empirical formulas to determine the resonance frequencies of the dominant modes of a crescent shaped dual-port microstrip antenna are developed. These calculations are validated by experimental results and the percentage error is found to be less than 2.

Acknowledgments: S.O. Kundukulam (Young collaborator programme) and C.K. Aanandan (Associate scheme) gratefully acknowledge the financial support and facilities provided by the Abdus Salam International Centre for Theoretical Physics (ICTP), Trieste, Italy.

11 March 2002
Electronics Letters Online No: 20020956
DOI: 10.1049/el:20020956

S.O. Kundukulam, M. Paulson, C.K. Aanandan, P. Mohanan and K.G. Nair (*Centre for Research in Electromagnetics and Antennas, Department of Electronics, Cochin University of Science and Technology, Cochin 682 022, India*)

E-mail: aanandan@doe.cusat.edu

References

1 KUNDUKULAM, S.O., PAULSON, M., AANANDAN, C.K., and MOHANAN, P.: 'Dual frequency dual polarised crescent-shaped microstrip antenna'. Proceedings of seventh national symposium on Antennas and Propagation, Cochin, 2000, pp. 90–93
2 DEEPUKUMAR, M., GEORGE, J., AANANDAN, C.K., MOHANAN, P., and NAIR, K.G.: 'Broadband dual frequency microstrip antenna', *Electron. Lett.*, 1996, **32**, pp. 1531–1532
3 BAHL, I.J., and BHARTIA, P.: 'Microstrip antennas' (Artech House, Dedham, MA, 1981)

Detection of microcalcifications in mammograms using local maxima and adaptive wavelet transform analysis

A.M. Bagci and A.E. Cetin

A method for computer-aided diagnosis of microcalcification clusters in mammogram images is presented. Microcalcification clusters which are an early sign of breast cancer appear as isolated bright spots in mammograms. Therefore they correspond to local maxima of the image. The local maxima of the image is first detected and they are ranked according to a higher-order statistical test performed over the subband domain data.

Introduction: Microcalcification clusters are an early sign of breast cancer. The survival rate approaches 100 per cent if cancer is detected early. Microcalcifications (MC) appear as isolated bright spots on mammograms images [1–4].

MCs correspond to local maxima of a mammogram as they are relatively bright and tiny regions in the image. The first step of our method is the detection of the local maxima of the mammogram image. Although a typical mammogram is much smoother than most natural images there are thousands of local maxima in a mammogram image. After detecting the maxima locations we rank them according to a higher-order statistical test performed over the subband domain data obtained by the adaptive wavelet transform. The distribution of wavelet data corresponding to the regular breast tissue is almost Gaussian [3, 4]. However, MCs are different in nature than regular breast tissue and they produce outliers in the subband domain. We take advantage of this fact and rank the local maxima according to a higher-order statistical test estimated in the neighbourhood of each local maximum. When the data is Gaussian the test statistics becomes zero. The higher the value of the test, the higher the rank of the maximum. Peaks due to MCs receive high ranks. The maxima due to small variations in the pixel values and smooth edges became low ranks.

We recently developed methods for detection of MCs based on higher-order statistics, and wavelet analysis [3, 4]. In these schemes the subband (or wavelet) domain image $|x_{lh}| + |x_{hl}| + |x_{hh}|$ of the mammogram image x is divided into overlapping small windows and a higher-order statistic (HOS) [5] is estimated in each window. The windows with HOS values higher than a threshold value T are marked as regions containing MC clusters. A weakness of the methods [3, 4] is that the threshold T should be estimated from a set of training images. The threshold has to be adjusted from scanner to scanner and according to the data set. In addition, we compute the HOS test only around maxima locations instead of the entire image, thus achieving a computationally more efficient method than [3, 4]. The HOS test is reviewed later in this Letter.

Another important feature of this Letter is that an adaptive wavelet (subband) transform [6] is used instead of a regular wavelet transform (WT). It is experimentally observed that adaptive WT provides better results than the ordinary Daubechies WT.

Adaptive wavelet transform: Classical adaptive prediction concepts are combined with the perfect reconstruction filter bank theory in [6] where the key idea is to decorrelate the polyphase components of the multichannel structure using an adaptive predictor P as shown in Fig. 1. Adaptation of the predictor coefficients are carried out by a least mean square (LMS)-type algorithm.

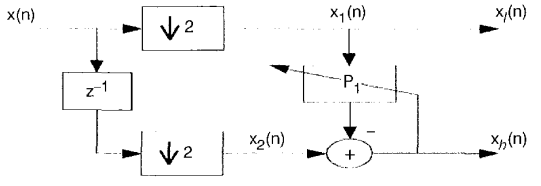

Fig. 1 *Analysis stage of two-channel adaptive filter bank structure (P_1 represents an adaptive predictor)*

In Fig. 1, $x_1(n)$ is the downsampled version of the original signal, $x(n)$, thus it consists of the even samples of $x(n)$. Similarly, the signal $x_2(n)$ consists of the odd samples. An LMS-based FIR predictor of $x_2(n)$ from $x_1(n)$ can be expressed as $\hat{x}_2(n) = \mathbf{w}(n)\mathbf{x}_1^T(n)$ where $\mathbf{x}_1(n) = [x_1(n-L), \ldots, x_1(n+L)]^T$ is the observation vector, and the $2L+1$ vector $\mathbf{w}(n)$ is the vector of predictor coefficients which is adapted by the equation

$$\mathbf{w}(n+1) = \mathbf{w}(n) + \mu \frac{\mathbf{x}_1(n)e(n)}{\|\mathbf{x}_1(n)\|^2} \quad (1)$$

where the error signal $e(n) = x_2(n) - \hat{x}_2(n)$.

The filterbank structure shown in Fig. 1 is the simplest adaptive wavelet transform (AWT) structure. In this structure, the 'highband signal' is essentially the prediction error and as a result the subsignals are expected to be decorrelated. Other AWT structures with antialising filters for the upper branch signal can be found in [6].

This one-dimensional filterbank is extended to two dimensions in a separable manner. The main advantage of the AWT over the standard WT is the use of adaptive prediction to compute the subimages x_{lh}, x_{hl}, and x_{hh}. Since MCs are isolated bright spots, they cannot be predicted using the background pixels corresponding to the breast tissue. As a result they produce outliers and the prediction error image pixels deviate from Gaussianity around MC locations. Conversely, background pixels corresponding to the breast tissue are very effectively estimated by the adaptive filter.

The downsampling operation in the AWT does not cause any data loss even if a MC consists of a single pixel. The AWT structure either tries to estimate this pixel by its neighbours or it is used in prediction of other pixels. In both cases it produces outliers in subimages as in the first case it cannot be predicted from its neighbours and in the second case it destroys the prediction process.

HOS test: The higher-order statistical (HOS) test used here is based on the sample estimates of the first four moments I_1, I_2, I_3, and I_4 of the wavelet data. Estimates of the moments are given by $I_k = 1/(M \times N) \sum_{m=1}^{M} \sum_{n=1}^{N} e^k[m, n]$, $k = 1, 2, 3, 4$ where $e = (|x_{lh}| + |x_{hl}| + |x_{hh}|)$. The subimages x_{lh}, x_{hl}, x_{hh} are obtained from the AWT of the mammogram image. In the limit $I_1 \to \mu$, $I_2 \to \sigma^2 + \mu^2$, $I_3 \to \mu^3 + 3\sigma^2\mu$ and $I_4 \to \mu^4 + 6\mu^2\sigma^2 + 3\sigma^4$, where μ and σ^2 denote the mean and the variance of the error e, respectively. As a result, the statistics

$$h_3(I_1, I_2, I_3) = I_3 - 3I_1(I_2 - I_1^2) - I_1^3 \quad (2)$$

and

$$h_4(I_1, I_2, I_4) = I_4 + 2I_1^4 - 3I_2^2 \quad (3)$$

are equal to zero for Gaussian distributed data in the limit. When there are outliers in the data, h and H deviate from zero. The test statistic used in this Letter is $H = h_3 + h_4$.

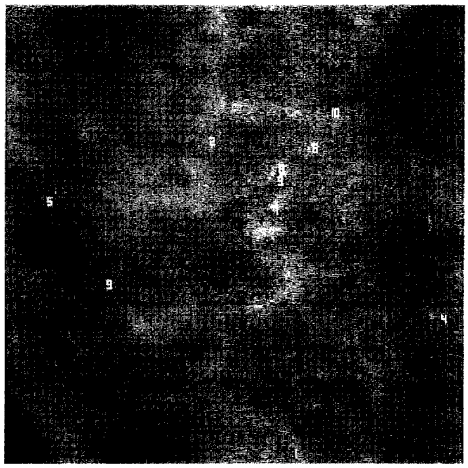

Fig. 2 *384 × 384 region of image c06c (peaks marked 3, 7, 8; 4; and 5, are microcalcifications)*

Detection method and experimental results: The detection algorithm consists of three steps. First, we analyse the mammogram image and detect the local maxima. We simply do this in two steps. We determine pixels with the property that $x(i, j) \geq x(i + l, j + k)$, $k, l = -2, -1, 1, 2$. We also divide the mammogram image into overlapping windows of size $M = 15 \times N = 15$ and determine the pixels which are greater than 5% of the mean of each block even if they do not satisfy the above condition. In a 2×2 K mammogram image we determine about 1000 candidate pixels for MC locations. In the second step we process the image using the analysis part of the AWT structure described in the second section of this Letter and we obtain the quarter size image $|x_{lh}| + |x_{hl}| + |x_{hh}|$. In the third step, we estimate the higher-order statistic, H, in an $M \times N$ window around each maximum location and the maxima are ranked according to their H value. A typical output image with the first 10 maxima is shown in Fig. 2.

Table 1: Ranks given to MCs by algorithm based on adaptive wavelet transform followed by HOS test (upper) and ordinary WT followed by HOS test (lower)

Image	Ranks given to microcalcifications		
	Region 1	Region 2	Region 3
c05o 2 regions	2	5	
	14, 19	121	
c06c 3 regions	5	3	4
	13	6	62
c07c 1 region	11		
	11, 15		
c08c 3 regions	2	11	4, 5
	1, 19	4, 5	13, 14
c09c 1 region	2		
	3		
c10c 1 region	3, 4		
	8, 11		
c13c 1 region	2		
	1, 4, 6		
c14c 2 regions	5	2, 3	
	13, 15	1	
c15c 1 region	3, 7		
	24		
c16c 1 region	2, 3		
	3, 4		
c18c 2 regions	1, 3	5	
	3, 4	11, 17	
c19c 2 regions	4	10	
	24	23	
c20c 1 region	4		
	35		

Detection results are summarised in Table 1 for 13 mammograms obtained from the Nijmegen University and University of Florida databases which have been studied by radiologists. For example, the image c05o has two regions containing MC clusters. The adaptive wavelet based method marks the MCs in the first (second) cluster as 2 (5) whereas in the wavelet transform based ranking the same MCs are ranked as 14 and 121, respectively. The AWT-based test produces better results in terms of ranking accuracy, as shown in Table 1.

In another experiment the maxima are ranked according to the variance around the maxima locations instead of the higher-order statistical (HOS) test. The average of ranks assigned to MC clusters by the AWT + HOS method is 4.28, while it is 9.6 in AWT and variance based ranking.

Radiologists can use the proposed method as a computer-aided diagnosis tool to obtain a second opinion or to verify their findings.

24 April 2002
Electronics Letters Online No: 20020907
DOI: 10.1049/el:20020907

A.M. Bagci and A. Enis (*Department of Electrical and Electronics Engineering, Bilkent University, Ankara, 06533, Turkey*)

E-mail: cetin@ee.bilkent.edu.tr

References

1 YOSHIDA, H., *et al.*: 'An improved computer-assisted diagnostic scheme using wavelet transform for detecting of clustered microcalcifications in digital mammograms', *Acad. Radiol.*, 1996, **3**, pp. 621–627
2 STRICTLAND, R.N., and HAHN, H.I.: 'Wavelet transforms for detecting microcalcifications in mammograms', *IEEE Trans. Med. Imag.*, 1996, **15**, pp. 218–229
3 GURCAN, M.N., YARDIMCI, Y., and CETIN, A.E.: 'Microcalcification detection using adaptive filtering and Gaussianity tests'. Proc. of 4th Int. Workshop on Digital Mammography, Nijmegen, The Netherlands, 1998, pp. 157–164
4 GÜRCAN, M.N., YARDIMCI, Y., ÇETIN, A.E., and ANSARI, R.: 'Detection of microcalcifications in mammograms using higher order statistics', *IEEE Signal Process. Lett.*, 1997, **4**, (8), pp. 213–216